Check for updates

Chemistry – An Asian Journal

CHEMISTRY AN ASIAN JOURNAL | ACES Asian Chemical Editorial Society

RESEARCH ARTICLE

Surface Structure, Thermal Behavior, and Electrochemical Stability of Oligo(ethylene glycol)-Terminated Alkanethiolate Self-Assembled Monolayers on Au(111)

Hyun Sun Sung[1] | Young Ji Son[1] | Jin Wook Han[1] | Hong Kyu Park[1] | Seo Yeon Park[1] | Keiko Hakata[2] | Motoharu Kimura[2] | Tomohiro Hayashi[2] | Jaegeun Noh[1,3]

[1]Department of Chemistry, Hanyang University, Seoul, South Korea | [2]Department of Materials Science and Engineering, School of Materials and Chemical Technology, Institute of Science Tokyo, Yokohama, Kanagawa, Japan | [3]Research Institute for Convergence of Basic Science, Hanyang University, Seoul, South Korea

Correspondence: Tomohiro Hayashi (th@mct.isct.ac.jp) | Jaegeun Noh (jgnoh@hanyang.ac.kr)

Received: 15 August 2026 | **Revised:** 10 October 2026 | **Accepted:** 19 October 2026

Keywords: adsorption state | adsorption | electrochemical stability | scanning tunneling microscopy | self-assembled monolayers | surface chemistry | surface structure

ABSTRACT

To investigate the effects of oligo(ethylene glycol) (OEG) chain length and thermal factors on the formation of self-assembled monolayers (SAMs), the surface structure, adsorption state, and electrochemical stability of SAMs of 2-[2-(2-methoxyethoxy)ethoxy]ethanethiol (EG3 SAMs) on Au(111) at an elevated temperature were examined using scanning tunneling microscopy (STM), x-ray photoelectron spectroscopy (XPS), and cyclic voltammetry (CV). To gain a clearer understanding, the results for EG3 SAMs were directly compared with those observed for decanethiolate (DT) SAMs. STM observations revealed that DT SAMs formed after deposition at 323 K for 2 and 24 h exhibited a well-ordered c(4 × 2) phase regardless of the deposition time, whereas EG3 SAMs at 323 K for 2 h displayed a mixed morphology of ordered and disordered phases containing brightly aggregated rows. After deposition at 323 K for 24 h, the brightly aggregated rows almost disappeared and more uniformly ordered SAMs were formed on the entire Au (111) surface. Moreover, CV measurements showed that EG3 SAMs are reductively desorbed from the Au surface much more easily than DT SAMs. In this study, we clearly demonstrated that the OEG backbone significantly affects the formation, surface structure, thermal behavior, and electrochemical stability of SAMs.

1 | Introduction

Surface and interfacial properties of metal surfaces can be readily controlled using self-assembled monolayers (SAMs) formed by adsorption of organic molecules while altering their head groups, molecular backbones, and terminal functional groups [1–12]. Therefore, SAMs can provide an excellent platform for various bio- and nano-related practical applications such as corrosion inhibition [13], biointerface [14], bioelectronics [15], batteries [16], solar energy devices [17, 18], and electronic devices [1, 19–21]. In particular, alkanethiolate SAMs have been extensively studied to understand their molecular self-assembly behaviors, surface structures, growth mechanism, physical, and chemical properties [2, 22–28]. Functionalized alkanethiolate SAMs are known to provide a simple and novel method for controlling the surface and interfacial properties of metal surfaces [2, 14, 22, 29]. Interestingly,

Hyun Sun Sung, Young Ji Son, and Jin Wook Han contributed equally to this work.

All rights reserved, including rights for text and data mining and training of artificial intelligence technologies or similar technologies.
© 2026 Wiley-VCH GmbH

oligo(ethylene glycol) (OEG)-terminated alkanethiolate SAMs on metals have been frequently applied in biomedical and biosensing fields because they can effectively inhibit nonspecific adsorption of proteins on the SAM surface [30–35]. Infrared absorption and x-ray photoelectron spectroscopy (XPS) measurements revealed that the methoxy-terminated tri(ethylene glycol) thiol SAMs on the Au surface had a mixed phase of crystalline helical and amorphous structures, whereas the SAM on the Ag surface had an all-trans conformation, which is interpreted to be due to differences in packing density depending on the metal type [32]. Additionally, OEG SAMs with a mixed phase were shown to effectively inhibit nonspecific protein adsorption. Interestingly, when the number of ethylene glycol $(EG)_n$ units n is equal to or greater than $n = 6$, OEG SAMs tend to form helical structures, whereas when n is less than 6, OEG SAMs are known to have a mixed conformation of helical and amorphous structures [32, 36, 37]. Meanwhile, compared to pure ethanol solution, a mixed solution of water and ethanol can achieve a higher packing density of hydroxy-terminated OEG SAMs ($n = 2$ or 4), and these SAMs exhibit higher protein adsorption properties [38]. The nonspecific adsorption properties were found to be significantly influenced by structural order, packing density, and conformation of the OEG SAMs [30–32, 35–38]. Therefore, it is particularly important to understand these issues both from the fundamental perspective of surface science and the practical applications based on OEG SAMs.

Several atomic force microscopy (AFM) and scanning tunneling microscopy (STM) studies have been performed to understand the molecular-scale features of the OEG SAMs on Au(111) surfaces [39–41]. AFM observations revealed the formation of closely packed and well-ordered domains of OH-$(EG)_6$-terminated alkanethiolate SAMs on Au(111) containing unique linear molecular depression [39]. High-resolution STM observations revealed that SAMs formed from CH_3-$(OCH_2CH_2)_2$-SH (n = 2; abbreviated as EG2 SAMs) on Au(111) in ethanol solutions have a mixed phase of ordered and disordered domains [40]. Additionally, the structural order of EG2 SAMs from vapor deposition increased with increasing deposition temperature [41]. Meanwhile, despite numerous STM studies to understand the molecular-scale surface structures and phase transitions of alkanethiolate SAMs on Au(111) with different alkyl chain lengths under various experimental conditions [2, 24–26, 42–48], only a few STM results for OEG SAMs have been reported to date, as mentioned above [40, 41].

Unlike previous studies on EG2 SAMs formed at room temperature [40] or by vapor deposition [41], this study focuses on SAMs derived from CH_3-$(OCH_2CH_2)_3$-SH ($n = 3$; abbreviated as EG3 SAMs) formed at an elevated temperature to investigate the effects of EG chain length and thermal factors on SAM formation and structure. The surface structure, adsorption state, and reductive desorption behavior of EG3 SAMs on Au(111) were investigated using STM, XPS, and cyclic voltammetry (CV). Additionally, to better understand the influence of the OEG backbone on SAM formation, these results were directly compared with those obtained for SAMs formed by decanethiol with a similar molecular length (DT SAMs). Figure 1 shows the chemical structures of DT and EG3 molecules and the formation of SAMs on Au(111) at an elevated temperature. In this study, we report the first molecular-scale STM results regarding the surface structure and thermal behavior of EG3 SAMs on Au(111), demonstrating that they differ completely from the results observed for DT SAMs.

2 | Experimental Section

2.1 | Chemicals

Decanethiol (C10SH) was purchased from Tokyo Chemical Industry Co., LTD (Tokyo, Japan). EG3 thiol (EG3SH) was synthesized using a method previously described in the literature [49]. The product was confirmed by ^{1}H NMR (400 MHz, $CDCl_3$): δ (ppm) 3.671–3.623 (m, 10H), 3.571–3.558 (s, 3H), 2.728–2.676 (m, 2H), and 1.612–1.570 (t, 1H). To eliminate the influence of water on the conformation of OEG group, an anhydrous grade of ethanol solvent was used for SAM formation.

2.2 | Preparation of Au(111) Substrates

Single-crystal Au(111) substrates were prepared by thermal evaporation of gold on mica sheets preheated at 623 K under ultrahigh vacuum conditions of 10^{-5}–10^{-6} Pa. STM imaging shows that the Au(111) substrates contain large, atomically flat terraces ranging from approximately 100–300 nm in size.

2.3 | Preparation of DT and EG3 SAMs

To better understand the formation and structure of EG3 SAMs, both DT and EG3 SAMs were prepared by immersing Au(111) substrates in 0.01 mM ethanol solutions of C10SH and EG3SH at 323 K for 2 and 24 h, respectively. Their surface structures, adsorption state, and electrochemical properties were then directly compared. The SAM-covered Au(111) substrates were removed from the solutions and thoroughly washed with pure ethanol to remove any physisorbed species. Subsequently, they were dried under a nitrogen gas stream before surface characterization.

2.4 | STM, XPS, and CV Measurements

STM measurements were performed with a NanoScope E (Veeco, Santa Barbara, CA, USA) using a commercial Pt/Ir (80:20) tips. All STM images were obtained in constant current mode in air at room temperature (RT). A bias voltage (V_b) of 180–300 mV and tunneling currents (I_t) of 0.30–0.50 nA for STM imaging were applied between the tip and the sample. XPS measurements were carried out using a Theta Probe (Thermo Fisher Scientific, U.K.). Monochromatic Al Kα radiation with an energy of 1486.6 eV was used as the x-ray source, and the emitted electrons were collected using a multichannel plate at angles ranging from 23° to 83°. The obtained spectra were calibrated to the binding energy of the Au $4f_{7/2}$ peak at 84.0 eV. The S 2p XPS peaks were determined by curve-fitting analysis using Voigt functions. CV measurements for reductive desorption (RD) were carried out using an electrochemical analyzer (CHI-600e Electrochemical Analyzer, CH instrument, inc. Bee Cave, USA). RD measurements were performed at a rate of 400 mV/s over a

18614731x, 2026, 21, Downloaded from https://acss.onlinelibrary.wiley.com/doi/10.1002/asia.71027 by Hanyang University Library, Wiley Online Library on [18/11/2026]. See the Terms and Conditions (https://onlinelibrary.wiley.com/terms-and-conditions) on Wiley Online Library for rules of use; OA articles are governed by the applicable Creative Commons License

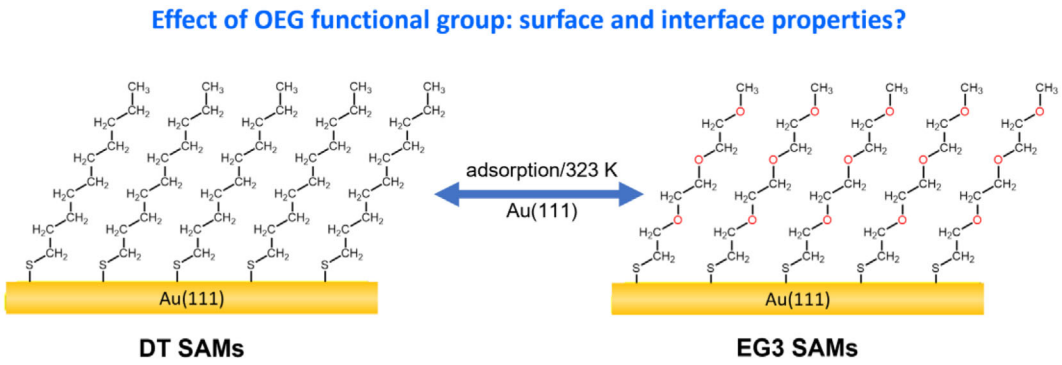


FIGURE 1 | Schematic diagram showing the formation of DT and EG3 SAMs on Au(111).

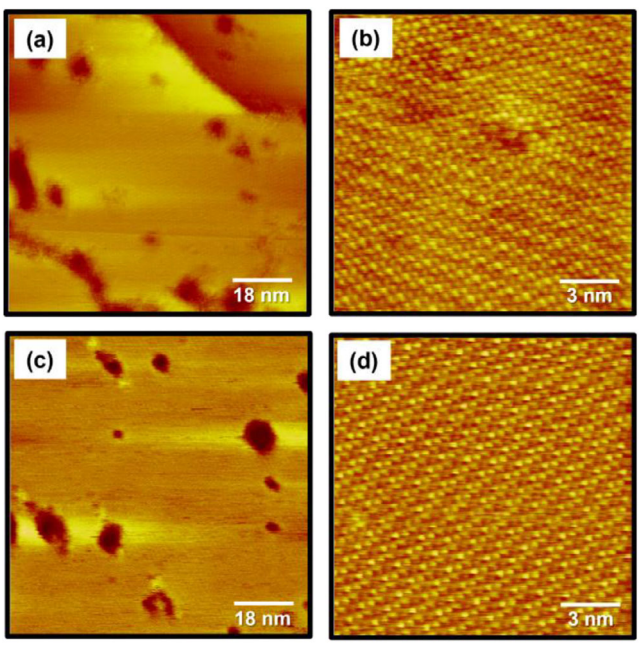


FIGURE 2 | STM images of DT SAMs on Au(111) in a 0.01 mM ethanol solution at 323 K for (a, b) 2 h and (c, d) 24 h. High-resolution STM images (b,d) show that closely packed and well-ordered DT SAMs with a c(4 × 2) packing structure are formed regardless of deposition time. The scan sizes of the STM images are (a,c) 90 nm × 90 nm and (b,d) 15 nm × 15 nm, respectively.

potentiometric range of 0 to −1200 mV in a 0.5 M KOH electrolyte solution degassed with nitrogen.

3 | Results and Discussion

To understand the effect of the OEG functional group on the formation and structure of SAMs on Au(111), it is very useful to directly compare the surface structures of OEG SAMs and alkanethiolate SAMs with a normal alkyl chain. Meanwhile, alkanethiolate SAMs on Au(111) formed at an elevated solution temperature were found to exhibit high structural order with large, well-ordered domains and few structural defects (e.g., vacancy islands and domain boundaries) [26, 28, 44, 50]. Therefore, in this study, DT and EG3 SAMs were prepared at an elevated solution temperature of 323 K. STM images in Figure 2 show surface morphology and molecular-scale feature of DT SAMs on Au(111) formed in 0.01 mM ethanol solution at 323 K for 2 h (Figure 2a and 2b) and 24 h (Figure 2c,d). Large-scale STM images (90 nm × 90 nm) in Figure 2a,c show that DT SAMs have a uniform surface structure containing vacancy islands (dark pits), which are usually observed in various alkanethiolate SAMs [2, 24–26, 28, 43–48]. On the other hand, molecular-scale STM images (15 nm × 15 nm) in Figure 2b,d clearly show that DT SAMs have well-ordered domains with a c(4 × 2) packing structure, which is commonly observed in closely packed alkanethiolate monolayers [2, 42, 44, 45, 47, 48, 50]. These results imply that well-ordered and closely packed DT SAMs were formed in 0.01 mM ethanol solution at 323 K regardless of deposition time. These results are supported by previous XPS and STM results showing that closely packed alkanethiolate SAMs with ($\sqrt{3} \times \sqrt{3}$)R30° or c(4 × 2) structures at saturation coverage were formed within 1 h in 0.1–0.001 mM ethanol solutions at RT [51]. Additionally, in situ STM observations revealed a formation of closely packed ($\sqrt{3} \times \sqrt{3}$)R30° phase for DT SAMs within 30 min–1 h (>0.005 mM solution) [52]. From this STM study, it was clearly demonstrated that adsorption of DT molecules on Au(111) in a 0.01 mM ethanol solution at 323 K for 2 or 24 h resulted in the formation of well-ordered and closely packed SAMs with the c(4 × 2) structures.

STM images in Figure 3 show surface features of EG3 SAMs on Au(111) in 0.01 mM ethanol solution at 323 K for 2 h. Interestingly, STM observations clearly revealed that the surface structure of EG3 SAMs was completely different from that of DT SAMs formed under the identical SAM preparation conditions. It was found that when DT molecules are adsorbed on Au (111), uniform and well-ordered SAMs with a c (4 × 2) domain structure are formed after deposition for 2 h (Figure 2a,b), whereas when EG3 molecules are adsorbed, non-uniform SAMs consisting of an ordered phase (region A), a disordered phase (region B), and brightly aggregated molecular rows (indicated by white arrows) are formed (Figure 3a,b). The STM observations clearly demonstrated that the surface characteristics of EG3 SAMs are very different from those of alkanethiolate SAMs. The most distinctive surface feature of EG3 SAMs is the formation of brightly aggregated rows (disordered rows) of varying lengths that are aligned in the same direction as the ordered molecular rows (Figure 3b). These results provide strong evidence that EG3 SAMs grow preferentially along a specific direction. In our previous STM study, a similar "bright molecular aggregate row" structure was observed in EG2 SAMs, even when the SAMs were formed at room temperature, regardless of the adsorption time [40]. These

1861471x, 2026, 21, Downloaded from https://aces.onlinelibrary.wiley.com/doi/10.1002/asia.71027 by Hanyang University Library, Wiley Online Library on [18/11/2026]. See the Terms and Conditions (https://onlinelibrary.wiley.com/terms-and-conditions) on Wiley Online Library for rules of use; OA articles are governed by the applicable Creative Commons License

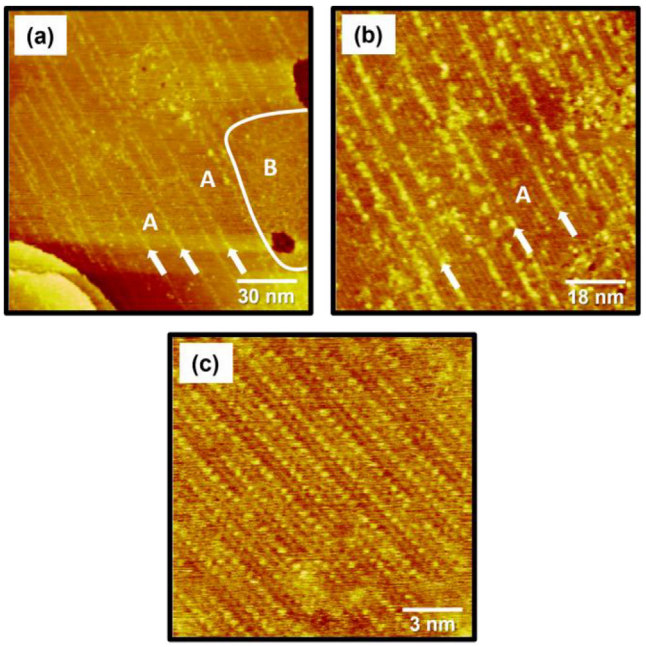


FIGURE 3 | STM images of EG3 SAMs on Au(111) formed by a 0.01 mM ethanol solution at 323 K for 2 h. STM images show that the surface features of EG3 SAMs containing several phases are significantly different from those of DT SAMs. The scan sizes of the STM images are (a) 150 nm × 150 nm, (b) 90 nm × 90 nm, and (c) 15 nm × 15 nm, respectively.

STM observations indicate that the "bright molecular aggregate row" structure is characteristic of thiolate SAMs containing OEG chains. Based on these findings, we propose that this unique structure, observed exclusively in EG3 SAMs, may originate from changes in molecular conformation induced by steric hindrance arising from the flexibility of the OEG chains and electrostatic repulsion between neighboring chains. Conformational changes in OEG chains have also been reported in several spectroscopic studies [32, 36, 37]. Magnified STM image (15 nm × 15 nm) in Figure 3c clearly reveals that the ordered phase indicated by A in Figure 3a,b are composed of ordered molecular rows. On the other hand, it is difficult to observe ordered molecules in region B and the bright aggregated rows in EG3 SAMs on Au(111). Interestingly, infrared adsorption and x-ray photoelectron spectroscopic studies of OEG SAMs revealed the coexistence of a crystalline ordered phase and an amorphous disordered phase [32]. Furthermore, near-edge x-ray absorption fine structure (NEXAFS) study has also suggested that OEG SAMs exhibit a mixed morphology comprising both crystalline and amorphous phases [36]. Our molecular-scale STM results clearly demonstrate the coexistence of a crystalline ordered phase and an amorphous disordered phase, which is good consistent with previous spectroscopic studies [32, 36].

Molecularly resolved STM image in Figure 4a shows that the ordered phase of EG3 SAMs on Au(111) formed in a 0.01 mM ethanol solution at 323 K for 2 h has a well-ordered molecular packing structure with alternating bright and dark molecular rows. Based on this STM image, the lattice parameters of a rectangular unit cell containing four molecules are: $a = 20.3 \pm 0.2$ Å $= 7a_h$, and $b = 5.0 \pm 0.2$ Å $= \sqrt{3}a_h$, where a_h is 2.89 Å, which corresponds to the interatomic spacing of the Au(111)

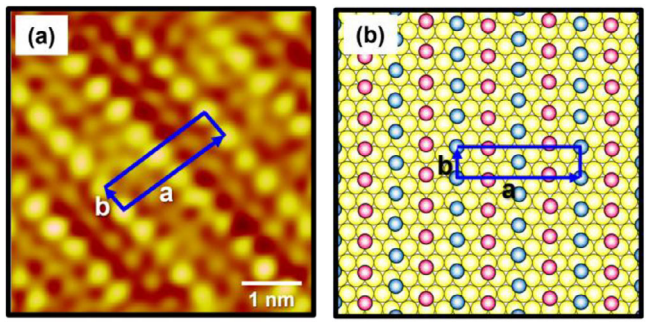


FIGURE 4 | (a) High-resolution STM image (5 nm × 5 nm) of EG3 SAMs on Au(111) in a 0.01 mM ethanol solution at 323 K for 2 h. (b) A proposed structural model of EG3 SAMs on Au(111).

lattice. Figure 4b shows a structural model of the ordered phase of EG3 SAMs on Au (111), which is assigned to a $(7 \times \sqrt{3})$ structure. In the proposed adsorption model, both the apparent molecular height and the adsorption-site stability reported in recent theoretical studies [51] were considered. Accordingly, the brighter molecular spots were assigned to bridge sites, whereas the darker molecular spots were assigned to three-fold hollow sites. The average area per molecule for EG3 SAMs was calculated to be 25.3 Å^2/molecule, which is slightly larger than that of closely packed alkanethiolate SAMs with a $(\sqrt{3} \times \sqrt{3})$R30° or c(4 × 2) structure (21.5 Å^2/molecule). This result means that OEG-terminated alkanethiolate SAMs are slightly loosely packed compared to alkanethiolate SAMs. Meanwhile, EG2 SAMs on Au(111) formed in a 1 mM solution at RT for 24 h were found to have a $(7 \times \sqrt{3})$ packing structure with two bright rows appearing repeatedly [45]. Although the adsorption patterns of EG2 and EG3 SAMs observed by STM are different, their packing structure and arial molecular density are identical. In this study, it was clearly demonstrated that EG2 and EG3 SAMs have very similar surface features with an ordered phase containing bright molecular aggregated rows and molecular packing structures. Therefore, these unique surface features can be considered as an intrinsic characteristic of OEG SAMs (EG2 or EG3 SAMs). On the other hand, STM studies for chain-length dependent SAM formation revealed that alkanethiol $(CH_3(CH_2)_{n-1}SH)$ with short alkyl chain length ($n < 6$) often form loosely packed SAMs with a $(p \times \sqrt{3})$ structure, whereas alkanethiol $(CH_3(CH_2)_{n-1}SH)$ with long alkyl chain length ($n \geq 6$) usually form closely packed SAMs with a well-known $(\sqrt{3} \times \sqrt{3})$R30° or c(4 × 2) structure regardless of the alkyl chain length [42–48, 50, 52–55]. In this study, it was clearly demonstrated that the surface structures of EG3 SAMs on Au(111) were completely different from those of alkanethiolate SAMs, suggesting that OEG terminal groups strongly affect the formation and structure of EG3 SAMs.

It is well known that deposition temperature and time are crucial factors in the formation and structure of alkanethiolate SAMs on Au(111) [26, 28, 44, 56]. Previous STM observations revealed that well-ordered DT SAMs with a c(4 × 2) structure were formed on the entire Au(111) surface at 333 K for 1 and 24 h [28, 44]. In contrast, when deposition was carried out at a higher temperature of 343 K for 24 h, DT SAMs consisted of two distinct phases consisting of a closely packed c(4 × 2) structure and a loosely packed (p × $\sqrt{3}$) structure. This is because high deposition temperature and long deposition time facilitated the

1861471x, 2026, 21, Downloaded from https://acces.onlinelibrary.wiley.com/doi/10.1002/asia.71027 by Hanyang University Library, Wiley Online Library on [18/11/2026]. See the Terms and Conditions (https://onlinelibrary.wiley.com/terms-and-conditions) on Wiley Online Library for rules of use; OA articles are governed by the applicable Creative Commons License

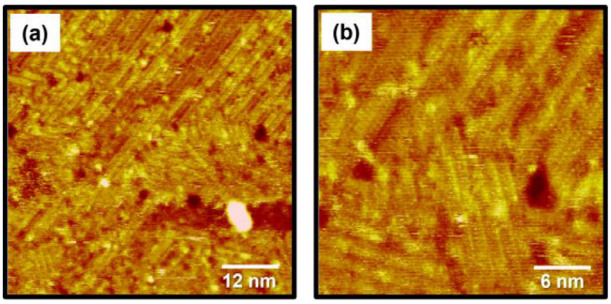


FIGURE 5 | STM images of EG3 SAMs on Au(111) in a 0.01 mM ethanol solution at 323 K for 24 h. STM images show that the brightly aggregated molecular rows have almost disappeared after prolonged deposition for 24 h. The scan sizes of STM images are (a) 60 nm × 60 nm and (b) 30 nm × 30 nm, respectively.

desorption of DT molecules from the SAMs [44]. Therefore, using an appropriate deposition time at high deposition time is very important for the fabrication of high-quality SAMs. As shown in Figure 2, STM observations also showed that well-ordered DT SAMs with few structural defects were formed across the entire surface of Au(111) after deposition at 323 K for 2 h or 24 h. This result is in good agreement with previous STM results for octanethiolate (OT) or DT SAMs [44, 56]. To understand the effect of deposition time on the formation of EG3 SAMs on Au(111) at 323 K, the deposition time was increased from 2 to 24 h. The STM images in Figure 5 show the surface features of EG3 SAMs on Au(111) formed in a 0.01 mM ethanol solution at 323 K for 24 h. The surface structures of the DT SAMs formed at 323 K for 2 and 24 h were almost identical regardless of the deposition time (Figure 2), but the surface structures of the EG3 SAMs changed remarkably. After deposition for a longer period of 24 h, the brightly aggregated rows (disordered phase) observed after 2 h deposition almost disappeared, and more uniformly ordered SAMs were formed across the entire surface of Au (111) (Figure 5a). However, the structural order of EG2 SAMs formed at room temperature did not improve even after prolonged deposition for 24 h [40]. These results suggest that the structural quality of EG3 SAMs can be significantly improved through the synergistic effects resulting from prolonged deposition at an elevated deposition temperature of 323 K for 24 h. Therefore, a sufficient deposition time at an elevated deposition temperature is essential for EG3 SAMs to form more uniform and ordered monolayers, which is driven by facile surface diffusion of adsorbed molecules. This process can lead to the optimization of interactions between OEG molecular backbones. The enlarged STM image (30 nm × 30 nm) in Figure 5b shows that the ordered domains of EG3 SAMs consist of ordered molecular rows, and the distance between adsorbed molecules in the rows was measured to be 5.0 ± 0.2 Å, which corresponds to $\sqrt{3}$ times the Au(111) lattice. STM observations revealed that the surface morphology of EG3 SAMs becomes more uniform after long-term deposition, but the structural order of EG3 SAMs does not significantly improve despite investigating many SAM samples. Therefore, considering the slightly lower surface coverage of the EG3 SAMs compared with DT SAMs (as demonstrated by STM and XPS results), steric hindrance arising from the flexibility of the OEG backbone and electrostatic repulsion between neighboring OEG chains are expected to hinder the formation of well-ordered EG3 SAMs with long-range order.

To understand the adsorption state of EG3 SAMs on Au(111), we compared the S 2p XPS spectra of DT and EG3 SAMs on Au(111) formed after deposition at 323 K for 24 h. STM observations revealed that the surface structures of DT and EG3 SAMs (Figures 2 and 5) were completely different from each other, whereas the S 2p XPS spectra of both SAMs were nearly identical, as shown in Figure 6. Three kinds of S 2p XPS peaks, designated as S1, S2, and S3, were observed, implying the presence of three different sulfur adsorption states in the SAMs. Note that each S 2p XPS peak consists of a doublet of $2p_{3/2}$ and $2p_{1/2}$ components with an intensity ratio of 2:1 due to spin–orbit splitting [55–58]. The $2p_{3/2}$ peaks for S1 and S2 were observed at approximately 161.4 and 162.2 eV, respectively; these peaks are assigned to the chemisorbed sulfur resulting from the formation of S-Au chemical bonds between the sulfur anchoring group and the Au surface. The S1 peak intensities of DT and EG3 SAMs were significantly weaker than the S2 peak intensities. The S1 peak is attributed to various factors, such as atomic sulfur [27], changes in sulfur hybridization resulting from variations in the adsorption orientation of the molecular backbone [57, 58], or effects associated with defects or step edges [59]. Interestingly, the intensity of S1 peak was observed to decrease as the structural order of octanethiol SAMs improved [56]. The S1 peak as a main peak was also often observed for poorly ordered SAMs [56–58]. Meanwhile, the S2 peak was observed as the main peak for the DT and EG3 SAMs. Indeed, such high-intensity peaks are commonly observed in well-ordered thiolate SAMs [55–57]. The STM results from this study, demonstrating the formation of ordered DT and EG3 SAMs, are in good agreement with the XPS results. In addition, the $2p_{3/2}$ peak for S3 with relatively weak intensity was observed at approximately 163.5 eV, which is attributed to physisorbed sulfur often observed in various organic thiolate SAMs [55, 58, 60]. Based on the Au 4f peak, the relative adsorption amounts of chemisorbed sulfur (S1 + S2) for DT and EG3 SAMs were measured to be 0.0049 and 0.0043, respectively. This indicates that the surface coverage of EG3 SAMs chemisorbed on Au(111) is approximately 12% more loosely packed than that of DT SAMs. XPS measurements showed that EG3 SAMs were mainly formed through chemisorption between sulfur atoms and the Au(111) surface.

CV measurements were performed to understand the electrochemical behaviors of EG3 SAMs by comparing those of DT SAMs. It is well known that the shape and position of the RD potential peaks of organic SAMs can provide meaningful information about structural quality, surface coverage, van der Waals interactions between molecular backbones, and binding characteristics between anchoring groups and metals [8, 61–64]. Figure 7 shows the RD behaviors of DT and EG3 SAM-modified Au(111) electrodes formed after deposition at 323 K for 24 h. The RD potential peaks of these SAMs were found to be significantly different from each other. The sharp RD potential peak of DT SAMs was observed at −1.09 V, whereas that of EG3 SAMs was observed at a much less negative potential of −0.86 V. This result means that EG3 molecules within SAMs are reductively desorbed from the Au surface much more easily than DT molecules. On the other hand, similar RD peaks ranging from −0.8 to −0.9 V were observed from well-ordered SAMs derived from alkanethiols with short alkyl chains such as propanethiol and butanethiol [61, 63, 64]. Therefore, the appearance of the RD peak for EG3 SAMs at a much less negative potential is attributed primarily to weak van der Waals interactions resulting

18614 1x, 2026, 21, Downloaded from https://acces.onlinelibrary.wiley.com/doi/10.1002/asia.71027 by Hanyang University Library, Wiley Online Library on [18/11/2026]. See the Terms and Conditions (https://onlinelibrary.wiley.com/terms-and-conditions) on Wiley Online Library for rules of use; OA articles are governed by the applicable Creative Commons License

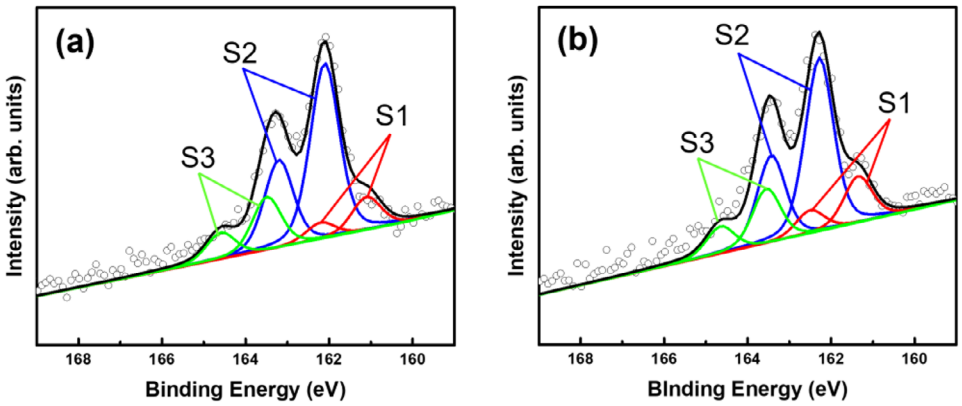


FIGURE 6 | S 2p XPS spectra of (a) DT and (b) EG3 SAMs on Au(111) in a 0.01 mM ethanol solution at 323 K for 24 h.

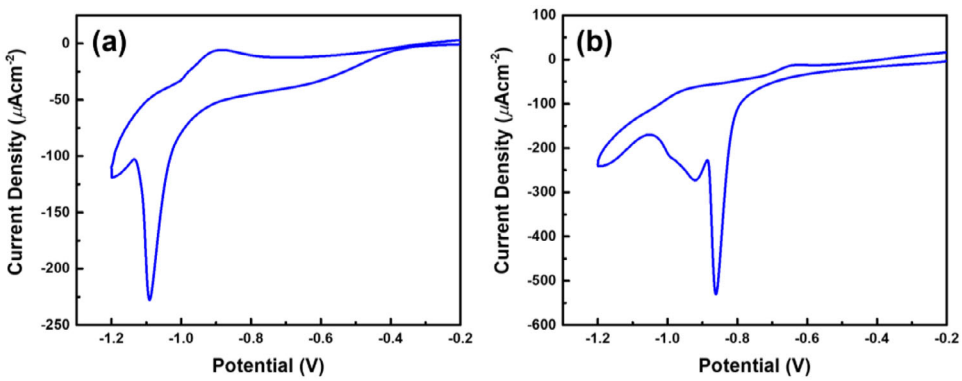


FIGURE 7 | CVs for RD of (a) DT and (b) EG3 SAM-modified Au working electrodes formed in a 0.01 mM ethanol solution at 323 K for 24 h. The CVs for RD were recorded by cycling at a rate of 0.4 V s^{-1} in the potential range of 0 to −1.2 V.

from electrostatic repulsion between the EG3 molecular backbones.

In contrast to DT SAMs with a sharp single peak, EG3 SAMs have a second broad RD peak around −0.92 V, which is probably due to the inhomogeneous phase of EG3 SAMs caused by OEG backbones, as shown in the STM images of Figure 5. Similarly, broad RD peaks were also observed in EG2 SAMs containing multiple molecular aggregates formed via vapor deposition [41]. This suggestion can be supported by the fact that various alkanethiolate SAMs with a well-ordered c(4 × 2) structure covered over the entire Au(111) surface exhibit only a sharp single RD peak [62, 63, 65], which is also demonstrated in this STM study on DT SAMs (Figure 2). Meanwhile, it was also reported that dodecanethiolate SAMs with inhomogeneous structural phases have two broad RD peaks at −0.671 and −0.946 [66]. From CV measurements, it was clearly demonstrated that the position and shape of RD peaks of EG3 SAMs were significantly different from DT SAMs, which is mainly due to the intrinsic surface and interface characteristics of EG3 SAMs on Au(111).

4 | Conclusions

The formation, surface structure, adsorption state, and electrochemical stability of DT and EG3 SAMs on Au(111) formed in a 0.01 mM ethanol solution at 323 K were characterized by STM, XPS, and CV. STM observations revealed that DT SAMs formed at 323 K for 2 and 24 h have well-ordered phase with a c(4 × 2) structure regardless of deposition time, whereas EG3 SAMs formed at 323 K for 2 h have several structural phases consisting of an ordered phase, a disordered phase, and brightly aggregated molecular rows. The ordered phase of EG3 SAMs can be described as a $(7 \times \sqrt{3})$ structure. After the deposition time increased to 24 h, the brightly aggregated molecular rows (disordered phase) observed after 2 h deposition almost disappeared, and more uniformly ordered SAMs were formed across the entire surface of Au (111). This result means that the structural quality of EG3 SAMs can be significantly improved after long-term deposition at 323 K for 24 h. XPS analysis revealed that adsorption states of DT and EG3 SAMs were nearly identical, and that these SAMs were formed through chemical interactions between the sulfur anchoring group and the Au(111) surface. Furthermore, CV results showed that the sharp RD potential peak of DT SAMs appeared at −1.09 V, whereas the sharp RD potential peak of EG3 SAMs appeared at −0.86 V, a much less negative potential. This means that EG3 molecules within SAMs are reductively desorbed from the Au surface much more easily compared to DT molecules. The results obtained here can provide new insights into understanding the surface structure, adsorption state, thermal behavior, and electrochemical stability of OEG-terminated SAMs on Au(111) surfaces.

1861471x, 2026, 21, Downloaded from https://acces.onlinelibrary.wiley.com/doi/10.1002/asia.71027 by Hanyang University Library, Wiley Online Library on [18/11/2026]. See the Terms and Conditions (https://onlinelibrary.wiley.com/terms-and-conditions) on Wiley Online Library for rules of use; OA articles are governed by the applicable Creative Commons License

Author Contributions

Hyun Sun Sung: methodology, investigation, data curation, and validation. **Young Ji Son:** methodology, investigation, and data curation. **Jin Wook Han:** resources and methodology. **Hong Kyu Park:** investigation. **Seo Yeon Park:** investigation. **Keiko Hakata:** resources. **Motoharu Kimura:** resources. **Tomohiro Hayashi:** writing – review and editing, supervision, and funding acquisition. **Jaegeun Noh:** conceptualization, writing – original draft, writing – review and editing, supervision, and funding acquisition.

Acknowledgments

This work was supported by the Basic Science Research Program through the National Research Foundation of Korea (NRF) funded by the Ministry of Education (2020R1A6A1A06046728, 2021R1A2C2010917, and 2024K2A9A2A08000126). This work was also supported by MEXT/JSPS KAKENHI Grant Numbers (JP26K01354) and was performed under the Research Program for CORE lab of "Five-star Alliance" in "NJRC Mater. & Dev." This work was also supported by the Japan–Taiwan Exchange Association, the Innovative Science and Technology Initiative for Security, and Acquisition, Technology & Logistics Agency (JPJ013268), Japan.

Conflicts of Interest

The authors declare no conflicts of interest.

Data Availability Statement

Data will be made available on request.

References

1. M. Li, M. Liu, F. Qi, F. R. Lin, and A. K.-Y. Jen, "Self-Assembled Monolayers for Interfacial Engineering in Solution-Processed Thin-Film Electronic Devices: Design, Fabrication, and Applications," *Chemical Reviews* 124 (2024): 2138–2204, https://doi.org/10.1021/acs.chemrev.3c00396.

2. J. C. Love, L. A. Estroff, J. K. Kriebel, R. G. Nuzzo, and G. M. Whitesides, "Self-Assembled Monolayers of Thiolates on Metals as a Form of Nanotechnology," *Chemical Reviews* 105 (2005): 1103–1170, https://doi.org/10.1021/cr0300789.

3. L. V. Romashov and V. P. Ananikov, "Self-Assembled Selenium Monolayers: From Nanotechnology to Materials Science and Adaptive Catalysis," *Chemistry—A European Journal* 19 (2013): 17640–17660, https://doi.org/10.1002/chem.201302115.

4. S. Seong, J. W. Han, G. Joo, H. S. Sung, H. K. Park, and J. Noh, "Formation, Structure, and Thermal Annealing Effects of Ordered Self-Assembled Monolayers of 4-Fluorobenzeneselenol on Au(111)," *Molecules* 30 (2025): 2057, https://doi.org/10.3390/molecules30092057.

5. J. Ossowski, G. Nascimbeni, T. Żaba, et al., "Relative Thermal Stability of Thiolate- and Selenolate-Bonded Aromatic Monolayers on the Au(111) Substrate," *Journal of Physical Chemistry C* 121 (2017): 28031–28042, https://doi.org/10.1021/acs.jpcc.7b09685.

6. S. Seong, H. Kang, H. Kim, et al., "Effects of the Substituent Position on the Structural Order, Work Function Change, and Thermopower of Dichloro-Substituted Benzenethiolate Self-Assembled Monolayers on Au(111)," *Applied Surface Science* 642 (2024): 158661, https://doi.org/10.1016/j.apsusc.2023.158661.

7. P. Cyganik, A. Terfort, and M. Zharnikov, "Odd-Even Effects in the Structure and Properties of Aryl-Substituted Aliphatic Self-Assembled Monolayers," *Nano Research* 17 (2024): 4231–4243, https://doi.org/10.1007/s12274-023-6292-8.

8. S. Han, J. W. Han, S. Seong, et al., "Formation and Structure of Highly Ordered Self-Assembled Monolayers on Au(111) via Vapor Deposition of Dioctyl Diselenides," *International Journal of Molecular Sciences* 26 (2025): 9192, https://doi.org/10.3390/ijms26189192.

9. J. Noh and M. Hara, "Structural Investigation of Cyclohexanethiol Self-Assembled Monolayers on Au(111) by Scanning Tunneling Microscopy," *Langmuir* 18 (2002): 9111–9115, https://doi.org/10.1021/la020342d.

10. R. Muneyasu, T. Yamada, M. Akai-Kasaya, and H. S. Kato, "Self-Assembly of Heterogeneous Bilayers Stratified by Au–S and Hydrogen Bonds on Au(111)," *Physical Chemistry Chemical Physics* 24 (2022): 22222–22230, https://doi.org/10.1039/D2CP03356A.

11. W. Azzam, A. Subaihi, N. A. F. Al-Rawashdeh, and A. Al-Nawaiseh, "Imaging of Terphenyldithiol Molecules in Highly Orientated and Ordered Aromatic Dithiol SAMs on Au(111)," *Journal of Physical Chemistry C* 128 (2024): 4093–4103, https://doi.org/10.1021/acs.jpcc.4c00102.

12. E. Ito, J. Noh, and M. Hara, "Different Adsorption States Between Thiophene and α-Bithiophene Thin Films Prepared by Self-Assembly Method," *Japanese Journal of Applied Physics* 42 (2003): L852–L855, https://doi.org/10.1143/JJAP.42.L852.

13. A. Salcı and R. Solmaz, "Fabrication of Rhodanine Self-Assembled Monolayer Thin Films on Copper: Solvent Optimization and Corrosion Inhibition Studies," *Progress in Organic Coatings* 125 (2018): 516–524, https://doi.org/10.1016/j.porgcoat.2018.09.020.

14. T. Hayashi and G. V. Latag, "Self-Assembled Monolayers as Platforms for Nanobiotechnology and Biointerface Research: Fabrication, Analysis, Mechanisms, and Design," *ACS Applied Nano Materials* 8 (2025): 8570–8587, https://doi.org/10.1021/acsanm.5c00790.

15. B. Lee, S. Takeda, K. Nakajima, et al., "Rectified Photocurrent in a Protein Based Molecular Photo-Diode Consisting of a Cytochrome b562-Green Fluorescent Protein Chimera Self-Assembled Monolayer," *Biosensors and Bioelectronics* 19 (2004): 1169–1174, https://doi.org/10.1016/j.bios.2003.11.016.

16. Z. Dai, S. K. Yadavalli, M. Chen, A. Abbaspourtamijani, Y. Qi, and N. P. Padture, "Interfacial Toughening With Self-Assembled Monolayers Enhances Perovskite Solar Cell Reliability," *Science* 372 (2021): 618–622, https://www.science.org/doi/10.1126/science.abf5602.

17. S. Y. Kim, S. J. Cho, S. E. Byeon, X. He, and H. J. Yoon, "Self-Assembled Monolayers as Interface Engineering Nanomaterials in Perovskite Solar Cells," *Advanced Energy Materials* 10 (2020): 2002606, https://doi.org/10.1002/aenm.202002606.

18. A. Mutlu, M. Can, and C. Tozlu, "Performance Improvement of Organic Solar Cell via Incorporation of Donor Type Self-Assembled Interfacial Monolayer," *Thin Solid Films* 685 (2019): 88–96, https://doi.org/10.1016/j.tsf.2019.05.064.

19. S. Casalini, C. A. Bortolotti, F. Leonardi, and F. Biscarini, "Self-Assembled Monolayers in Organic Electronics," *Chemical Society Reviews* 46 (2017): 40–71, https://doi.org/10.1039/C6CS00509H.

20. M. M. Thuo, W. F. Reus, C. A. Nijhuis, et al., "Odd−Even Effects in Charge Transport Across Self-Assembled Monolayers," *Journal of the American Chemical Society* 133 (2011): 2962–2975, https://doi.org/10.1021/ja1090436.

21. H. Lee, H. Kim, D. Kim, et al., "Correlation Between the Electrical Properties and Formation Temperature of Self-assembled Monolayer-Based Molecular Junctions," *ACS Nano* 19 (2025): 36223–36231, https://doi.org/10.1021/acsnano.5c07611.

22. C. Vericat, M. E. Vela, G. Benitez, P. Carro, and R. C. Salvarezza, "Self-Assembled Monolayers of Thiols and Dithiols on Gold: New Challenges for a Well-Known System," *Chemical Society Reviews* 39 (2010): 1805, https://doi.org/10.1039/b907301a.

23. H. Wu, G. Li, J. Hou, and K. Sotthewes, "Probing Surface Properties of Organic Molecular Layers by Scanning Tunneling Microscopy," *Advances in Colloid and Interface Science* 318 (2023): 102956, https://doi.org/10.1016/j.cis.2023.102956.

24. E. Pensa, L. M. Azofra, T. Albrecht, R. C. Salvarezza, and P. Carro, "Shedding Light on the Interfacial Structure of Low-Coverage

18614171x, 2026, 21, Downloaded from https://acces.onlinelibrary.wiley.com/doi/10.1002/asia.71027 by Hanyang University Library, Wiley Online Library on [18/11/2026]. See the Terms and Conditions (https://onlinelibrary.wiley.com/terms-and-conditions) on Wiley Online Library for rules of use; OA articles are governed by the applicable Creative Commons License

Alkanethiol Lattices," *Journal of Physical Chemistry C* 124 (2020): 26748–26758, https://doi.org/10.1021/acs.jpcc.0c07613.

25. G. E. Poirier and E. D. Pylant, "The Self-Assembly Mechanism of Alkanethiols on Au(111)," *Science* 272 (1996): 1145–1148, https://doi.org/10.1126/science.272.5265.1145.

26. N. S. Lee, D. Kim, H. Kang, D. K. Park, S. W. Han, and J. Noh, "Structural Transitions of Octanethiol Self-Assembled Monolayers on Gold Nanoplates After Mild Thermal Annealing," *Journal of Physical Chemistry C* 115 (2011): 5868–5874, https://doi.org/10.1021/jp111506v.

27. A. Asyuda, S. Das, and M. Zharnikov, "Thermal Stability of Alkanethiolate and Aromatic Thiolate Self-Assembled Monolayers on Au(111): An X-ray Photoelectron Spectroscopy Study," *Journal of Physical Chemistry C* 125 (2021): 21754–21763, https://doi.org/10.1021/acs.jpcc.1c06984.

28. R. Yamada, H. Wano, and K. Uosaki, "Effect of Temperature on Structure of the Self-Assembled Monolayer of Decanethiol on Au(111) Surface," *Langmuir* 16 (2000): 5523–5525, https://doi.org/10.1021/la991394e.

29. P. Bhadra and S. W. I. Siu, "Effect of Concentration, Chain Length, Hydrophobicity, and an External Electric Field on the Growth of Mixed Alkanethiol Self-Assembled Monolayers: A Molecular Dynamics Study," *Langmuir* 37 (2021): 1913–1924, https://doi.org/10.1021/acs.langmuir.0c03414.

30. S. Herrwerth, W. Eck, S. Reinhardt, and M. Grunze, "Factors That Determine the Protein Resistance of Oligoether Self-Assembled Monolayers—Internal Hydrophilicity, Terminal Hydrophilicity, and Lateral Packing Density," *Journal of the American Chemical Society* 125 (2003): 9359–9366, https://doi.org/10.1021/ja034820y.

31. R. Valiokas, S. Svedhem, M. Östblom, S. C. T. Svensson, and B. Liedberg, "Influence of Specific Intermolecular Interactions on the Self-Assembly and Phase Behavior of Oligo(ethylene glycol)-Terminated Alkanethiolates on Gold," *Journal of Physical Chemistry B* 105 (2001): 5459–5469, https://doi.org/10.1021/jp004441g.

32. P. Harder, M. Grunze, R. Dahint, G. M. Whitesides, and P. E. Laibinis, "Molecular Conformation in Oligo(ethylene glycol)-Terminated Self-Assembled Monolayers on Gold and Silver Surfaces Determines Their Ability to Resist Protein Adsorption," *Journal of Physical Chemistry B* 102 (1998): 426–436, https://doi.org/10.1021/jp972635z.

33. L. Kankate, U. Werner, A. Turchanin, A. Gölzhäuser, H. Großmann, and R. Tampé, "Protein Resistant Oligo(ethylene glycol) Terminated Self-Assembled Monolayers of Thiols on Gold by Vapor Deposition in Vacuum," *Biointerphases* 5 (2010): 30–36, https://doi.org/10.1116/1.3407483.

34. Y. Mizuta, T. Onodera, P. Singh, K. Matsumoto, N. Miura, and K. Toko, "Development of an Oligo(ethylene glycol)-Based SPR Immunosensor for TNT Detection," *Biosensors and Bioelectronics* 24 (2008): 191–197, https://doi.org/10.1016/j.bios.2008.03.042.

35. T. Hayashi, Y. Tanaka, Y. Koide, M. Tanaka, and M. Hara, "Mechanism Underlying Bioinertness of Self-Assembled Monolayers of Oligo(ethyleneglycol)-Terminated Alkanethiols on Gold: Protein Adsorption, Platelet Adhesion, and Surface Forces," *Physical Chemistry Chemical Physics* 14 (2012): 10196, https://doi.org/10.1039/c2cp41236e.

36. M. Zwahlen, S. Herrwerth, W. Eck, M. Grunze, and G. Hähner, "Conformational Order in Oligo(ethylene glycol)-Terminated Self-Assembled Monolayers on Gold Determined by Soft X-ray Absorption," *Langmuir* 19 (2003): 9305–9310, https://doi.org/10.1021/la0350610.

37. P. S. Johnson, M. Goel, N. L. Abbott, and F. J. Himpsel, "Helical Versus All-Trans Conformations of Oligo(ethylene glycol)-Terminated Alkanethiol Self-Assembled Monolayers," *Langmuir* 30 (2014): 10263–10269, https://doi.org/10.1021/la500978s.

38. L. Li, S. Chen, J. Zheng, B. D. Ratner, and S. Jiang, "Protein Adsorption on Oligo(ethylene glycol)-Terminated Alkanethiolate Self-Assembled Monolayers: The Molecular Basis for Nonfouling Behavior," *Journal of Physical Chemistry B* 109 (2005): 2934–2941, https://doi.org/10.1021/jp0473321.

39. N. Inada, H. Asakawa, Y. Matsumoto, and T. Fukuma, "Molecular-Scale Surface Structures of Oligo(ethylene glycol)-Terminated Self-Assembled Monolayers Investigated by Frequency Modulation Atomic Force Microscopy in Aqueous Solution," *Nanotechnology* 25 (2014): 305602, https://doi.org/10.1088/0957-4484/25/30/305602.

40. H. Kang, S. Han, S. Seong, et al., "Unique Mixed Phases and Structures of Self-Assembled Monolayers on Au(111) Derived From Methoxy-Terminated Mono(ethylene glycol)Ethanethiols," *Journal of Physical Chemistry C* 121 (2017): 18021–18029, https://doi.org/10.1021/acs.jpcc.7b05817.

41. Y. J. Son, H. Kang, S. Seong, S. Han, N.-S. Lee, and J. Noh, "Thermally Driven Structural Order of Oligo(ethylene glycol)-Terminated Alkanethiol Monolayers on Au(111) Prepared by Vapor Deposition," *Molecules* 27 (2022): 5377, https://doi.org/10.3390/molecules27175377.

42. Q. Guo and F. Li, "Self-Assembled Alkanethiol Monolayers on Gold Surfaces: Resolving the Complex Structure at the Interface by STM," *Physical Chemistry Chemical Physics* 16 (2014): 19074, https://doi.org/10.1039/C4CP00596A.

43. X. Xiao, B. Wang, C. Zhang, Z. Yang, and M. M. T. Loy, "Thermal Annealing Effect of Alkanethiol Monolayers on Au(111) in Air," *Surface Science* 472 (2001): 41–50, https://doi.org/10.1016/S0039-6028(00)00920-1.

44. W. Azzam and L. A. Al-Momani, "A New Striped-Phase of Decanethiol Self-Assembled Monolayers on Au(111) Formed at a High Solution Temperature," *Applied Surface Science* 266 (2013): 239–244, https://doi.org/10.1016/j.apsusc.2012.11.162.

45. G. Poirier and M. J. Tarlov, "The c(4X2) Superlattice of n-Alkanethiol Monolayers Self-Assembled on Au(111)," *Langmuir* 10 (1994): 2853–2856, https://doi.org/10.1021/la00021a001.

46. G. Poirier, M. J. Tarlov, and H. E. Rushmeier, "Two-Dimensional Liquid Phase and the Px.sqroot.3 Phase of Alkanethiol Self-Assembled Monolayers on Au(111)," *Langmuir* 10 (1994): 3383–3386, https://doi.org/10.1021/la00022a004.

47. G. E. Poirier, "Coverage-Dependent Phases and Phase Stability of Decanethiol on Au(111)," *Langmuir* 15 (1999): 1167–1175, https://doi.org/10.1021/la981374x.

48. J. Noh and M. Hara, "Final Phase of Alkanethiol Self-Assembled Monolayers on Au(111)," *Langmuir* 18 (2002): 1953–1956, https://doi.org/10.1021/la010803f.

49. D. J. Keddie, J. B. Grande, F. Gonzaga, M. A. Brook, and T. R. Dargaville, "Amphiphilic Silicone Architectures via Anaerobic Thiol–Ene Chemistry," *Organic Letters* 13 (2011): 6006–6009, https://doi.org/10.1021/ol202051y.

50. A. H. A. Mamun and J. R. Hahn, "Effects of Solvent on the Formation of Octanethiol Self-Assembled Monolayers on Au(111) at High Temperatures in a Closed Vessel: A Scanning Tunneling Microscopy and X-ray Photoelectron Spectroscopy Study," *Journal of Physical Chemistry C* 116 (2012): 22441–22448, https://doi.org/10.1021/jp307940g.

51. E. Ventura-Macias, P. M. Martinez, R. Pérez, and J. G. Vilhena, "Quantum Mechanical Derived (VdW-DFT) Transferable Lennard–Jones and Morse Potentials to Model Cysteine and Alkanethiol Adsorption on Au(111)," *Advanced Materials Interfaces* 11 (2024): 2400369, https://doi.org/10.1002/admi.202400369.

52. M. Kawasaki, T. Sato, T. Tanaka, and K. Takao, "Rapid Self-Assembly of Alkanethiol Monolayers on Sputter-Grown Au(111)," *Langmuir* 16 (2000): 1719–1728, https://doi.org/10.1021/la990310z.

53. Y. Yamada and K. Uosaki, "In Situ Scanning Tunneling Microscopy Observation of the Self-Assembly Process of Alkanethiols on Gold(111) in Solution," *Langmuir* 14 (1998): 855–861, https://doi.org/10.1021/la970974d.

54. C. A. Alves, E. L. Smith, and M. D. Porter, "Atomic Scale Imaging of Alkanethiolate Monolayers at Gold Surfaces With Atomic Force Microscopy," *Journal of the American Chemical Society* 114 (1992): 1222–1227, https://doi.org/10.1021/ja00030a015.

18614 1x, 2026, 21, Downloaded from https://acces.onlinelibrary.wiley.com/doi/10.1002/asia.71027 by Hanyang University Library, Wiley Online Library on [18/11/2026]. See the Terms and Conditions (https://onlinelibrary.wiley.com/terms-and-conditions) on Wiley Online Library for rules of use; OA articles are governed by the applicable Creative Commons License

55. J. Noh, S. Jang, D. Lee, et al., "Abnormal Adsorption Behavior of Dimethyl Disulfide on Gold Surfaces," *Current Applied Physics* 7 (2007): 605–610, https://doi.org/10.1016/j.cap.2006.12.007.

56. A. H. A. Mamun and J. R. Hahn, "Effects of Immersion Temperature on Self-Assembled Monolayers of Octanethiol on Au(111)," *Surface Science* 606 (2012): 664–669, https://doi.org/10.1016/j.susc.2011.12.007.

57. T. Ishida, M. Hara, I. Kojima, et al., "High Resolution X-ray Photoelectron Spectroscopy Measurements of Octadecanethiol Self-Assembled Monolayers on Au(111)," *Langmuir* 14 (1998): 2092–2096, https://doi.org/10.1021/la971104z.

58. T. Ishida, N. Choi, W. Mizutani, et al., "High-Resolution X-Ray Photoelectron Spectra of Organosulfur Monolayers on Au(111): S(2p) Spectral Dependence on Molecular Species," *Langmuir* 15 (1999): 6799–6806, https://doi.org/10.1021/la9810307.

59. M. M. Walczak, C. A. Alves, B. D. Lamp, and M. D. Porter, "Electrochemical and X-Ray Photoelectron Spectroscopic Evidence for Differences in the Binding Sites of Alkanethiolate Monolayers Chemisorbed at Gold," *Journal of Electroanalytical Chemistry* 396 (1995): 103–114, https://doi.org/10.1016/0022-0728(95)04056-T.

60. D. G. Castner, K. Hinds, and D. W. Grainger, "X-Ray Photoelectron Spectroscopy Sulfur 2p Study of Organic Thiol and Disulfide Binding Interactions With Gold Surfaces," *Langmuir* 12 (1996): 5083–5086, https://doi.org/10.1021/la960465w.

61. C. A. Widrig, C. Chung, and M. D. Porter, "The Electrochemical Desorption of n-Alkanethiol Monolayers From Polycrystalline Au and Ag Electrodes," *Journal of Electroanalytical Chemistry and Interfacial Electrochemistry* 310 (1991): 335–359, https://doi.org/10.1016/0022-0728(91)85271-P.

62. N. Arisnabarreta, G. D. Ruano, M. Lingenfelder, E. M. Patrito, and F. P. Cometto, "Comparative Study of the Adsorption of Thiols and Selenols on Au(111) and Au(100)," *Langmuir* 33 (2017): 13733–13739, https://doi.org/10.1021/acs.langmuir.7b03038.

63. R. C. Salvarezza and P. Carro, "The Electrochemical Stability of Thiols on Gold Surfaces," *Journal of Electroanalytical Chemistry* 819 (2018): 234–239, https://doi.org/10.1016/j.jelechem.2017.10.046.

64. , "Reductive Desorption of Carboxylic-Acid-Terminated Alkanethiol Monolayers From Au(111) Surfaces," *Journal of Electroanalytical Chemistry* 428 (1997): 33–38, https://doi.org/10.1016/S0022-0728(97)00006-5.

65. O. Azzaroni, M. E. Vela, H. Martin, A. Hernández Creus, G. Andreasen, and R. C. Salvarezza, "Electrodesorption Kinetics and Molecular Interactions at Negatively Charged Self-Assembled Thiol Monolayers in Electrolyte Solutions," *Langmuir* 17 (2001): 6647–6654, https://doi.org/10.1021/la010019v.

66. Y. Choi, S. Seong, Y. J. Son, et al., "Formation of Long-Range-Ordered Self-Assembled Monolayers of Dodecyl Thiocyanates on Au(111) via Ambient-Pressure Vapor Deposition," *Colloids and Surfaces A: Physicochemical and Engineering Aspects* 583 (2019): 123969, https://doi.org/10.1016/j.colsurfa.2019.123969.

18614 1x, 2026, 21, Downloaded from https://acces.onlinelibrary.wiley.com/doi/10.1002/asia.71027 by Hanyang University Library, Wiley Online Library on [18/11/2026]. See the Terms and Conditions (https://onlinelibrary.wiley.com/terms-and-conditions) on Wiley Online Library for rules of use; OA articles are governed by the applicable Creative Commons License